Removal of Cadmium from Aqueous Streams by Zeolite Synthesized from Fly Ash

Gaurav Das[1], N. C. Pradhan[2], G. M. Madhu[1], H. S. Preetham[1]

[1]*Department of Chemical Engineering, M.S. Ramaiah Institute of Technology, Bangalore-560054, India*
[2]*Department of Chemical Engineering, Indian Institute of Technology, Kharagpur-721302, India*

Abstract

Zeolite was synthesised from fly ash collected from a power plant of Neyveli Corporation, Chennai, India. The synthesised zeolite was characterized using SEM, XRD, and FT-IR. Experiments were conducted to determine the feasibility of using the synthesized zeolite for the adsorption of cadmium using batch technique. The effect of time, dosage, temperature and pH on the adsorption was investigated. The equilibrium data was also collected and applied to the well-known adsorption isotherms of Langmuir, Freundlich and Dubinin–Kaganer–Radushkevich (DKR) model. The data perfectly fits all the models. From Dubinin–Kaganer–Radushkevich (DKR) adsorption model, the mean energy of sorption (E) has been evaluated and found to be 40-70 kJ mol^{-1} which is characteristic of an ion-exchange mechanism.

Keywords: Zeolite, Coal Fly Ash (CFA), Cadmium, Adsorption.

1. Introduction

Coal combustion produces a lot of inorganic residues in coal fired power plants which leads to a large amount of combustion by-products chiefly fly ash, bottom ash and slag. A lot of alternative methods are explored and put in action for the treatment of Coal Fly Ash (CFA), as cement supplement; this is because CFA is pozzolanic in nature [1]. When there are no feasible economic options, they are generally land filled [2]. CFA could also be used in the neutralization of acid mine drainage [3]. Conversion of CFA to zeolite is one of the potential alternatives for handling the CFA. The conversion of CFA to zeolite has twin benefits i.e. it fetches more value when compared to construction supplement and it is often used as catalyst and ion-exchanger in industries as it constitutes of higher contents of silica and alumina, which are the basic in the formation of zeolite. Earlier studies demonstrated the success in the conversion of CFA to zeolite [3-5]. Zeolite is widely used in several applications such as catalysts for hydrogenation, alkylation, isomerization and sorbents for the removal of contaminants such as heavy metals, toxic gases, dyes, and organic pollutants [4]. Generally, there are two major methods in the synthesis of zeolite from CFA: hydrothermal and fusion methods, these include classic alkaline conversion of fly ash by molten salt method [5].

The presence of traces of heavy metals in the aquatic environment has been of great concern because of their toxicity and non-biodegradable nature [6–8]. Heavy metals like cadmium also occurs in nature and is found to be associated with zinc minerals [9-11]. Studies have shown that cadmium is very toxic, because the human body lacks a homeostatic control for this metal. Moreover, cadmium is an enzyme inhibitor with potential to damage kidney and liver of animal species [12-13]. This metal is also used in a wide variety of industries such as plating, cadmium–nickel battery, phosphate fertilizers, mining, pigments, stabilizers and alloys [14-16] and finds its way to the aquatic environment through wastewater discharges. Based on the above, a systematic study on removal of cadmium from contaminated water is of considerable significance from an environmental point of view.

A number of methods are available for the removal of metal ions from aqueous solutions. They are ion exchange, solvent extraction, reverse osmosis, precipitation and adsorption. Activated carbon adsorption is a well-known method for the removal of heavy metals [17–19], but the high cost of activated carbon restricts its large-scale use for the abatement of heavy metal pollution in developing countries. Previously lot of researchers have used different adsorbents, developed from various industrial waste materials, for the removal

of heavy metals, such as synthesising activated carbon from waste rice husk, waste plastics, use of natural zeolites etc. [20–38]. Still there exists a need to develop a low cost and efficient adsorbent for the removal of cadmium from contaminated water. For sorption applications, zeolites were often reported to exhibit high sorption capacity, sorption affinity, and cation exchange capacity for divalent sorbates. Lee et al. [39] reported that the synthesized zeolite from CFA had greater adsorption capabilities for Pb^{2+} than the original fly ash (6–7 times) and natural zeolite (3–5 times). Erdem et al. [40] reported that natural zeolite hold great potential for the sorption of several heavy metal cations, e.g. $(Co^{2+}, Cu^{2+}, Zn^{2+} and\ Mn^{2+})$ and this could be used as alternative for activated carbon.

In the present study, an attempt has been made to develop an inexpensive adsorbent system by converting CFA into zeolite for the removal of toxic heavy metals such as cadmium from wastewater. Cadmium was selected because of its toxic nature to humans and also due to the exclusive study for the removal of cadmium by the synthesised zeolite has rarely been reported.

2. Materials and methods
2.1. Chemicals, sorbent material and instruments
All the chemicals and reagents used were of analytical grade and were obtained from E. Merck, India. Stock solutions of cadmium were prepared using cadmium nitrate in distilled water. pH meter (Systronics, India) was used for pH measurements. X-ray measurements were made using a Phillips X-ray diffractometer employing CuKα radiation. IR spectra of the samples were recorded on an infrared spectrophotometer (FTIR Perkin Elmer model 1600). SEM images of zeolite samples were taken by ZEISS. Cadmium concentration was analysed using Atomic Absorption Spectrometer (GBC 932 plus).

2.2. Fly ash collection
Coal fly ash sample was collected from electrostatic precipitators of Neyveli Lignite Corporation Ltd, Chennai, India. The samples contained both amorphous (mainly SiO_2, Al_2O_3) and crystalline components (mainly quartz and mullite). The physical and chemical properties of the fly ash samples used in the present investigation were characterized from EDAX analysis. The fly ash sample used was of 'Class F' type with SiO_2, Al_2O_3 and iron oxide as the major constituents. Different oxide concentrations of coal fly ash and zeolite were found using EDAX analysis.

2.3. Preparation of adsorbent material
The composition of raw fly ash was Na_2O-0.35%, MgO-2.4%, Al_2O_3-26.76%, SiO_2-39.2%, CaO-23.75%, Fe_2O_3-4.25% and TiO_2-3.25%. Raw fly ash samples were screened through a BSS Tyler sieve of 80-mesh size to remove the larger particles. Sodium hydroxide and fly ash were mixed in 1:1 ratio, milled and fused in a stainless steel tray at 550°C for 1 h. The resultant fused mixture was then cooled to room temperature, grounded further and added to water (10 g fly ash/100 mL water). The slurry thus obtained was agitated mechanically in a glass beaker for 12 h. It was then kept at around 100 °C for 6 h without any disturbance. The resultant precipitate was then repeatedly washed with distilled water to remove excess sodium hydroxide, filtered and dried. The sodium hydroxide added to the fly ash not only works as an activator, but also adjusts the sodium content in the starting material. Mullite and α- quartz present in the fly ash are the sources of aluminium and silicon, respectively, for zeolite formation. The synthesized zeolite was found to contain Na_2O-30.34%, MgO-1.48%, Al_2O_3-23.19%, SiO_2-40.67% , CaO-0.9%, TiO_2-0.63% and Fe_2O_3-3.64%.

3. Experimental
3.1. Preparation of stock solution
An aqueous solution of 100 mg L^{-1} Cd^{2+} was prepared by dissolving analytical grade cadmium nitrate $Cd(NO_3)_2.H_2O$ (E. Merck) in distilled water. pH of the solutions was maintained using H_2SO_4 and NaOH (AR grade, E. Merck).

3.2. Adsorption studies
Batch adsorption experiments were carried out in series of beakers (150 mL) and covered with glass sheets to prevent contamination, where the zeolite used was in the powder form. The effect of contact time (0-60 min), pH (2-8), adsorbent dosage (1-20 g L^{-1}) and temperature (30, 40, 45 and 50 °C) on the adsorption of cadmium on zeolite was investigated. The mean of three readings were considered and the average has been reported.

Percentage removal has been calculated for all the studied parameters using Equation 1 and equilibrium concentration on the adsorbent was calculated using Equation 2.

$$\% \operatorname{Re} moval = \frac{(C_i - C_f)}{C_i} X \ 100 \tag{1}$$

Where C_i = initial metal concentration in (mg L^{-1}), C_f = final metal concentration in (mg L^{-1})

$$q_e = \frac{(C_i - C_f)V}{M} \tag{2}$$

Where V= volume of reacting solution (L), M=amount of zeolite in solution (g), q_e = mass of metal adsorbed per unit mass of zeolite at time t (mg g^{-1}).

3.3. Zeolite regeneration
Regeneration of zeolite was tested by conducting successive adsorption/desorption cycles. 1M NaCl solution was used for desorption process. Once desorption process had reached equilibrium, the mineral was gently washed to remove the desorbing solution from its surface, it was then dried at 80°C and placed in a desiccator until the next adsorption/desorption cycle. During each adsorption/desorption cycle no other treatment took place in order to minimize the overall cost of the treatment process. Then repeated cycles were conducted for all liquid media under examination. After completion of each adsorption/desorption cycle the regenerated samples were used for further adsorption and desorption.

4. Results and discussion
4.1. Characterisation of synthesised zeolite
The synthesised zeolite was characterized using XRD, FT-IR and SEM. The cadmium adsorbed zeolite was characterized using SEM to check the change in surface morphology.

4.1.1. XRD Analysis
The X-Ray diffraction (XRD) patterns of the synthesised zeolite were obtained using a Philips X-ray diffractometer. Operating conditions involved the use of Cu-Kα radiation. The samples were scanned from 10–70° (2θ, where θ is the angle of diffraction). XRD analysis gives a measure of purity and crystallinity of the sample as shown in Figure 1. Quantitative measure of the crystallinity of the synthesized zeolite was found out by taking sum of major peaks height in XRD pattern. The percentage crystallinity was taken as the sum of the peak heights of the unknown materials divided by the sum of the peak heights of a standard material that has been assumed to be 100% crystalline. Percentage crystallinity of the sample was determined using the Equation 3. The crystallinity of the synthesized zeolite was 71%:

$$\% \ Crystallinity = \frac{(Sum \ of \ the \ peak \ heights \ of \ unknown \ material)}{(Sum \ of \ peak \ heights \ of \ s \tan dard \ material)} X \ 100 \tag{3}$$

The composition of the sample was determined from the standard JCPDS (Joint Committee of Powder Diffraction Standard) data. Peak at 26.6 represents Al_2O_3 reflection plane (0 1 2); JCPDS file 89-3072, Peak at 26.6 represents CaO_2 reflection plane (1 0 1); JCPDS file 85-0514, Peak at 26.6 represents SiO_2 reflection plane (3 1 2); JCPDS file 89-5416, Peak at 20.76 represents Na_2O_2 reflection plane (0 0 1); JCPDS file 74-0111, Peak at 32.22 represents Fe_3O_4 reflection plane (1 0 0); JCPDS file 89-6466, Peak at 54.82 represents Na_2O reflection plane (0 0 2); JCPDS file 89-5954, Peak at 59.92 represents Na_2O_2 reflection plane (2 2 0); JCPDS file 74-0895. The presence of non-stoichiometric oxides of calcium and sodium (i.e. CaO_2 and Na_2O_2) in the synthesized zeolite is evident from the composition determined from the JCPDS files. The presence of these non-stoichiometric oxides decreases the crystallinity of the synthesized zeolite.

4.1.2. SEM Analysis
The SEM (Scanning Electron Microscopy) images were taken using ZEISS EVO 60 with Oxford EDS detector. Figures 2 and Figure 3 represent scanning electron micrograph of synthesized zeolite and cadmium adsorbed zeolite. From Figure 3, we can observe that adsorption of cadmium on the zeolite in the form of lumps. The larger spheres are the zeolite structures whereas the smaller spherical structures spread all over is

the adsorbed cadmium. The space between two adsorbed cadmium over zeolite surface varies from 862.2nm to 1.297 micron as observed from this image.
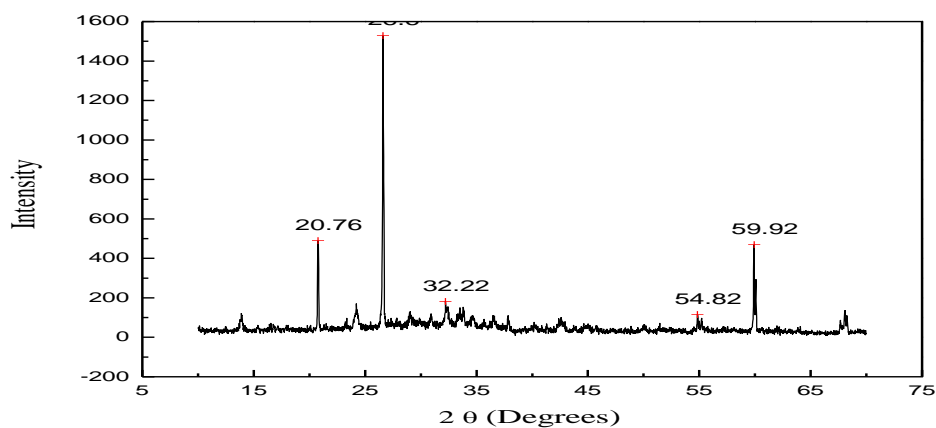
Figure 1: XRD pattern of the synthesized zeolite
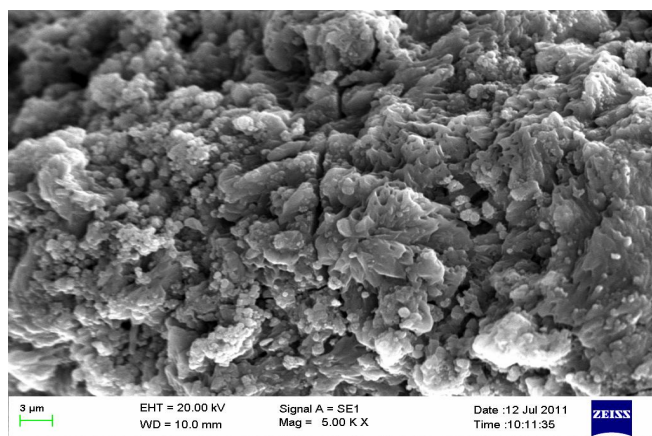
Figure 2: SEM image of the synthesised zeolite   **Figure 3:** SEM image of the cadmium adsorbed zeolite
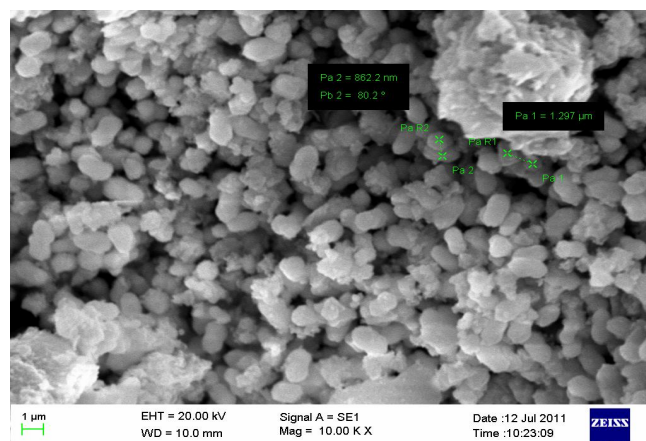
4.1.3. FT-IR Analysis

The IR spectrum of synthesised zeolite was taken in the range of 400-4000 cm^{-1} and recorded using Perkin Elmer spectrophotometer (Figure 4). Comparison of IR spectral data for the synthesized zeolite and NaX zeolite as reported by Flanigen et al., [41] are tabulated in Table 1. From the data it was observed that, synthesised zeolite is nearly having the same composition as that of NaX synthetic zeolite.

4.2. Adsorption studies
4.2.1. Effect of adsorbent dosage and time on cadmium removal

The adsorption capacity of cadmium on zeolite was tested by varying zeolite dosage (0.1 g, 0.5 g, 1.0 g and 2.0 g in 100 mL) in 100 mg L^{-1} cadmium concentration solution at pH 7. The solution was subjected to adsorption at ambient temperature (25±3°C). The suspensions were shaken at 200 rpm. Concentration of cadmium was estimated at regular intervals of time (5-30 min) using Atomic Absorption Spectrometer (AAS). The effect of time on cadmium adsorption is shown in Figure 5. Maximum adsorption was reached within first 15 min for all the adsorbent loadings. At 15 min, the cadmium adsorption efficiency for 0.1 g, 0.5 g, 1.0 g and 2.0 g are 29.45%, 55.45%, 68.92% and 73.37% respectively.

Adsorption efficiency (percentage adsorption) increases with an increase in the adsorbent dosage. The plot of percentage adsorption versus different adsorbent dosage after 30 min of adsorption at pH 7 is shown in Figure 6. An increase in the zeolite dosage increases the number of active sites which enables greater adsorption efficiency. With increased loading, the removal efficiency increases and finally saturates at 73.37% removal at 20 g L^{-1} zeolite loading.
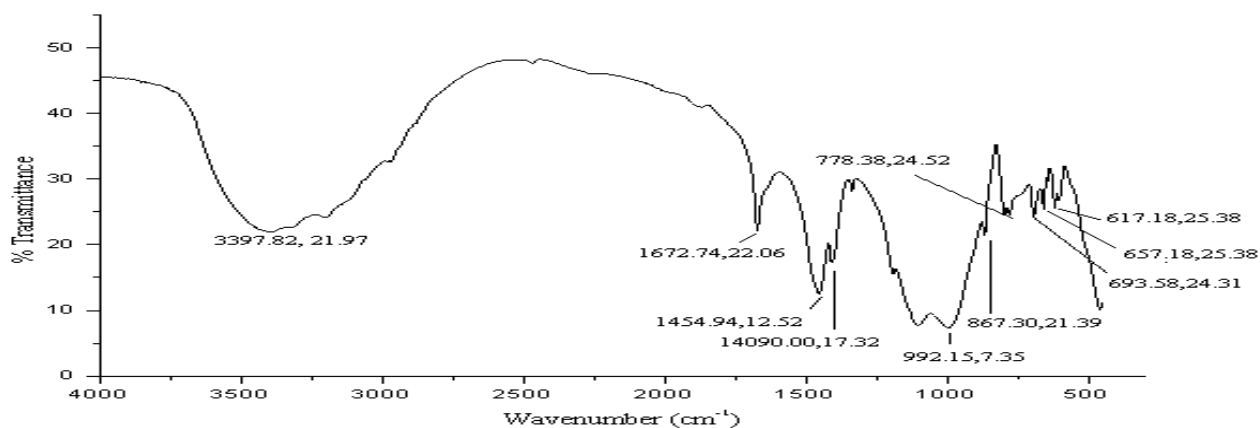
Figure 4: FT-IR of the synthesised zeolite

Table 1: Infrared spectral data for the synthesized zeolite and NaX zeolite

Parameter	Wave number (cm^{-1})	
	Synthesized zeolite	NaX [41]
Double ring	562 m	560 m
Asymmetric stretching (Si-O)	1088 msh, 986 s, 830 m	1060 msh, 971 s, 746 m
Symmetric Stretching (Si-O-Al)	665 m	668 m
T-O bending (Si-O)	452 s	458 ms
Pore opening	410 s	406 w

s = strong; ms = medium strong; m = medium; w = weak; sh= shoulder
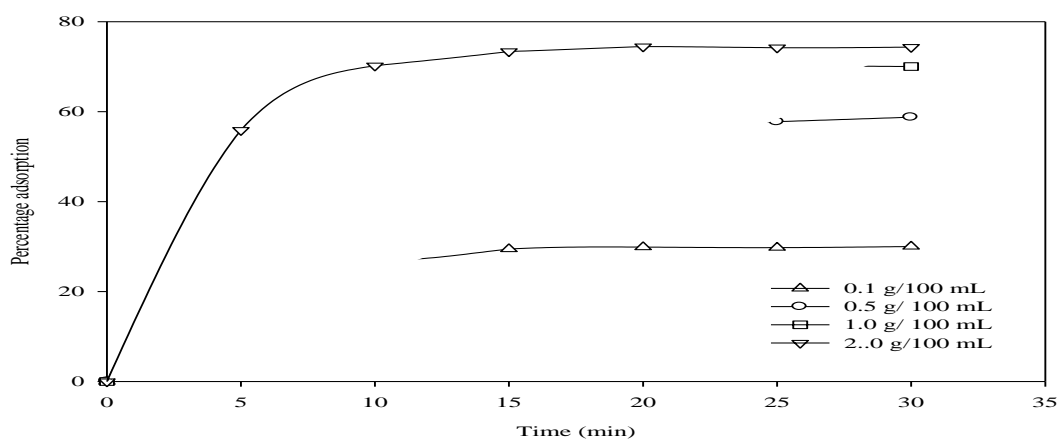
Figure 5: Effect of time on the adsorption of cadmium for different zeolite loadings at pH 7
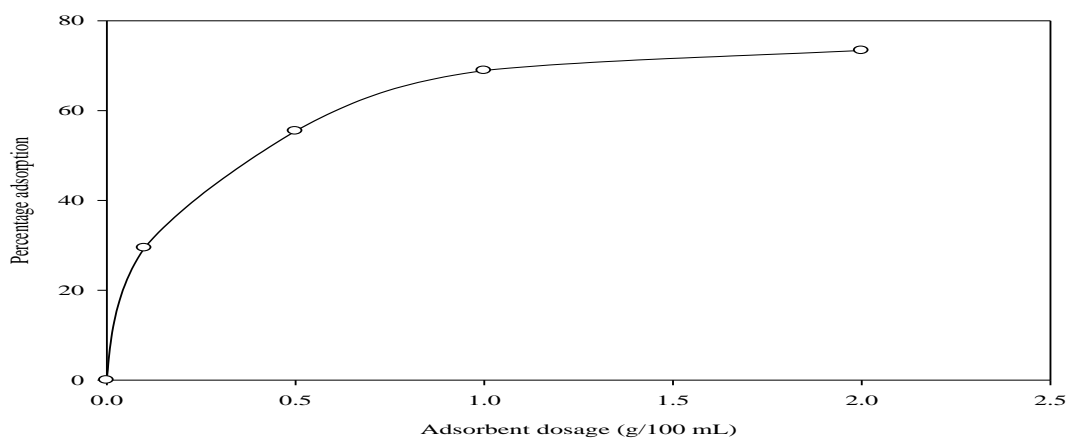
Figure 6: Effect of adsorbent dosage on the adsorption at pH 7

4.2.2. Effect of pH on cadmium removal

To study the effect of pH, experiments were carried out at fixed zeolite concentration (1.0 g of zeolite in 100 mL solution) by maintaining 100 mg L^{-1} cadmium concentration. The solution was stirred and analysed for cadmium concentration after 30 min at different pH. The adsorption of cadmium on zeolite was conducted in the pH range of 2-10. The effect of pH on the adsorption is shown in Figure 7. Adsorption efficiency increases with an increase in the pH and reaches the maximum at pH 6 with 80% removal. Further increase in pH decreases adsorption efficiency; a similar behaviour has been reported by Vinod et al. [2]. The decrease in the adsorption at higher pH may be attributed to the hydrolysis of cadmium [42].
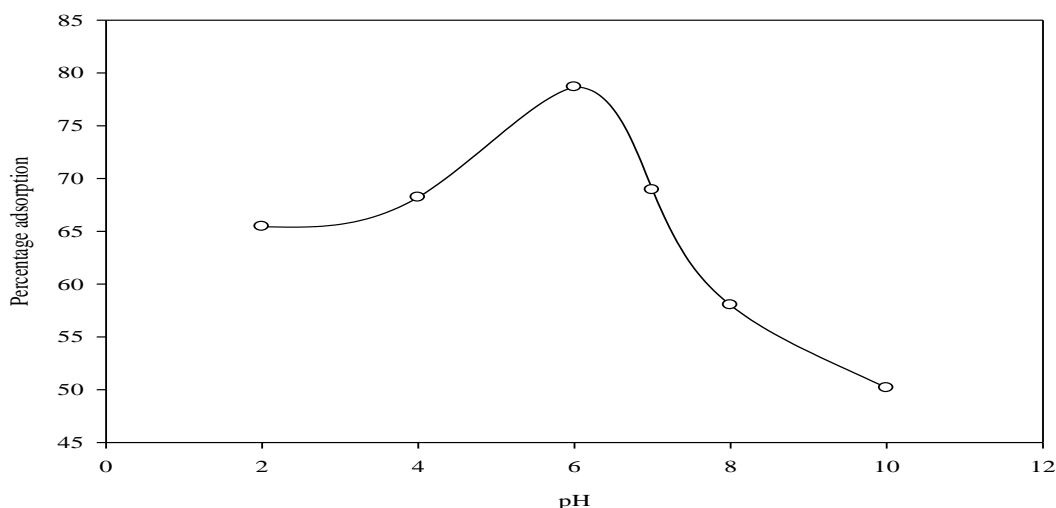
Figure 7: Effect of pH on the adsorption at an adsorbent dosage of 1.0 g/100 mL

4.2.3. Effect of temperature on cadmium removal

To study the effect of temperature on adsorption, experiments were carried out at fixed zeolite dosage (1.0 g of zeolite in 100 mL solution) by using100 mg L^{-1} cadmium concentration solution at 30, 40, 45, 50 and at 60 °C. pH of the solution was maintained at 7. Adsorption was carried out for 30 min. The effect of temperature on adsorption is shown in Figure 8. It could be observed that temperature has a profound effect on adsorption. It is observed that adsorption increases with an increase in temperature and maximum removal efficiency of 87.47 is achieved at 40 °C after which removal efficiency gradually decreases. There was a large increase in adsorption from 30 °C to 40 °C, from 72.4% to 87.47%. This may be explained based on the exothermic nature of the adsorption process. The process was highly effective at 40 °C and a further increase in temperature suppresses the adsorption affinity [43]. Same types of results have been reported by Borah and Senapati [44] for the adsorption of cadmium onto pyrite surface. The temperature may alter factors such as rate of adsorption, hydrolysis, recrystallization reactions and dissociation constants of water [45].
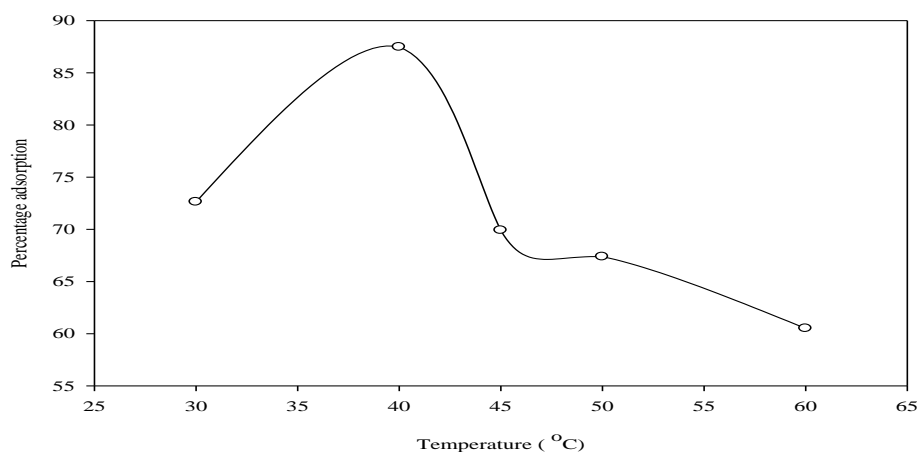
Figure 8: Effect of temperature on the adsorption at an adsorbent dosage of 10g L^{-1} and at pH 7

4.3. Adsorption isotherms

The results obtained by the adsorption of cadmium was analysed by the well-known models of Langmuir, Freundlich and Dubinin–Kaganer–Radushkevich (DKR).

4.3.1. Langmuir adsorption isotherm

Langmuir adsorption was used by many researchers for the sorption of a variety of compounds. The Langmuir isotherm is based on the assumption that there are uniform energies of adsorption onto the surface and no transmigration of adsorbate in the plane of the surface [2]. Adsorption occurs at specific homogeneous sites within the adsorbent. The linear form of Langmuir adsorption is given by Equation 4.

$$\frac{1}{Q_e} = \frac{1}{Q_0} + \frac{1}{bQ_0C_e} \tag{4}$$

Where Q_e (mg g^{-1}) is the adsorbed amount of cadmium, C_e (mg L^{-1}) is the equilibrium concentration of the cadmium in solution, Q_0 is the monolayer adsorption capacity, and b is the constant related to the free energy of adsorption. The values of Q_0 and b were calculated by plotting $\frac{1}{Q_0}$ versus $\frac{1}{C_e}$ with the intercept $\frac{1}{Q_0}$ and slope $\frac{1}{bQ_0}$ as shown in the Figure 9. All the data perfectly fit to Langmuir adsorption isotherm model.

The value of Q_0 and b at different temperatures has been tabulated (Table 2). An increase in temperature increases the adsorption till 40 °C; further increase in temperature then decreases the adsorption. There is maximum adsorption at 40 °C. At this temperature there is maximum activation of the active sites throughout the zeolite structure which enables maximum adsorption of cadmium, which is also evident from previous studies [43, 44] .The value of Q_0 = 13.45 mg g^{-1} is maximum at 40 °C. The temperature change affects parameters such as adsorption rate, hydrolysis, recrystallization reactions and dissociation constants of water [45] which is responsible for this kind of deviation at 40 °C.

Table 2: Langmuir adsorption constants and regression values at different temperatures

T (^{o}C)	B	Q_0	R^2
30	0.6492	2.7831	0.9473
40	0.2611	5.6211	0.9896
50	0.6849	2.6281	0.9255
60	1.1920	2.1034	0.9083
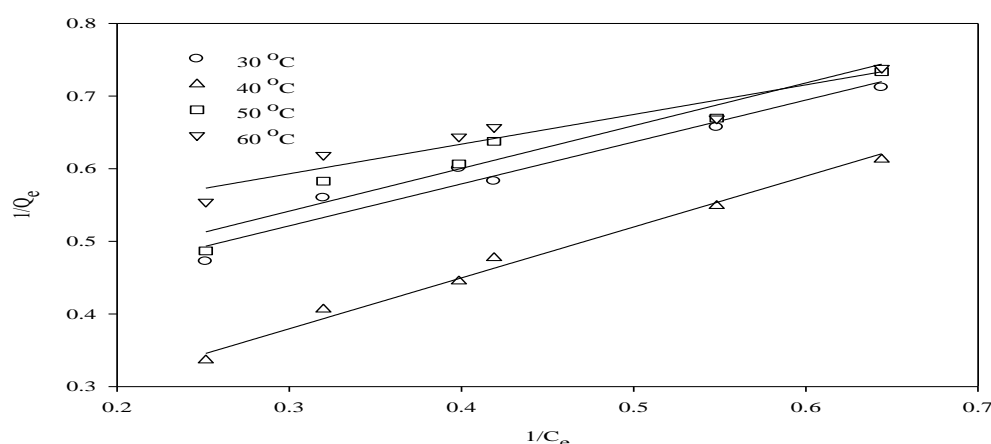
Figure 9: Langmuir isotherm for cadmium adsorption on zeolite at different temperatures

4.3.2. Freundlich adsorption isotherm

The adsorpion data of cadmium was analysed by Freundlich model. The logarithmic form of Freundlich model is given by the Equation 5 [42].

$$\ln Q_e = \ln K_f + \frac{1}{n} \ln C_e \tag{5}$$

Where Q_e = amount adsorbed (mg g^{-1}), C_e = equilibrium concentration of the adsorbate (mg L^{-1}) and K_f (mg g^{-1}) and n are Freundlich constants related to adsorption capacity and adsorption intensity, respectively. The plots of log Q_e against $\ln C_e$; for the adsorption data of cadmium is shown in Figure 10. The data is fitting very well to the Freundlich model. The constants for the Freundlich model for different temperatures are tabulated (Table 3). However, the Freundlich constants K_f and n were calculated from the best-fit lines. The n value is greater than one showing zeolite is a good adsorbent for the adsorption of cadmium [46].
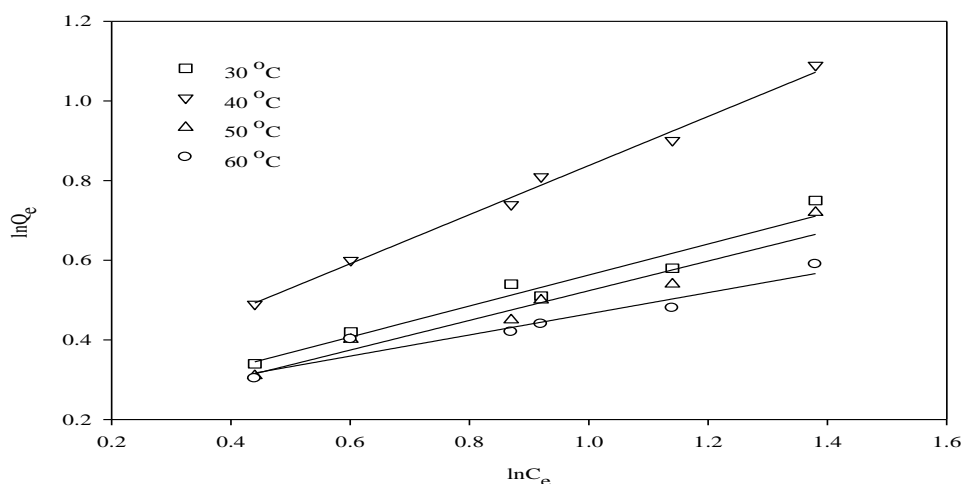
Figure 10: Freundlich isotherm for the cadmium adsorption on zeolite at different temperatures

Table 3: Freundlich adsorption constants and regression values at different temperatures

T (^{o}C)	1/n	K_f	R^2
30	0.4015	1.1796	0.9575
40	0.6212	1.2433	0.9926
50	0.3951	1.1439	0.9457
60	0.2654	1.2244	0.9291

4.3.3. Dubinin–Kaganer–Radushkevich (DKR) adsorption isotherm
Dubinin–Kaganer–Radushkevich (DKR) adsorption isotherm was verified for the adsorption of cadmium on zeolite in between 30 – 60 °C. DKR equation is based on the heterogeneous surface of the adsorbent which could be expressed in Equation 6.

$$\ln Q_e = \ln X_m - \beta \varepsilon^2 \tag{6}$$

Where, Q_e= adsorbed amount of cadmium (mg g^{-1}), X_m= maximum sorption capacity (mol g^{-1}), β = activity coefficient (mol^2 J^{-2}), the Polanyi potential which can be calculated using the Equation 7 [47-48].

$$\varepsilon = RT \ln(1 + \frac{1}{C_f}) \tag{7}$$

Where, ε = Polanyi potential, R = gas constant (0.00831447 KJ K^{-1} mol^{-1}) T = temperature (K), C_f = liquid-phase sorbate concentration at equilibrium (mg L^{-1}). Figure 11, the plot of lnQ versus ε^2 gives slopes (β) and intercepts (X_m), the values of which is tabulated in Table 4. The DKR adsorption constants are given in Table 4. In order to evaluate the nature of interaction between cadmium and the binding sites, the mean energy of sorption, E is calculated from the relationship: $E = \dfrac{1}{\sqrt{-2\beta}}$ The calculated E values for zeolite are 50 and

40.8248 kJ mol^{-1} at 30 °C (303 K) and at 40 °C (313 K) respectively, which lie in the range of energies (40–70 kJ mol^{-1}) characteristic for the ion-exchange mechanisms [14, 47-48].
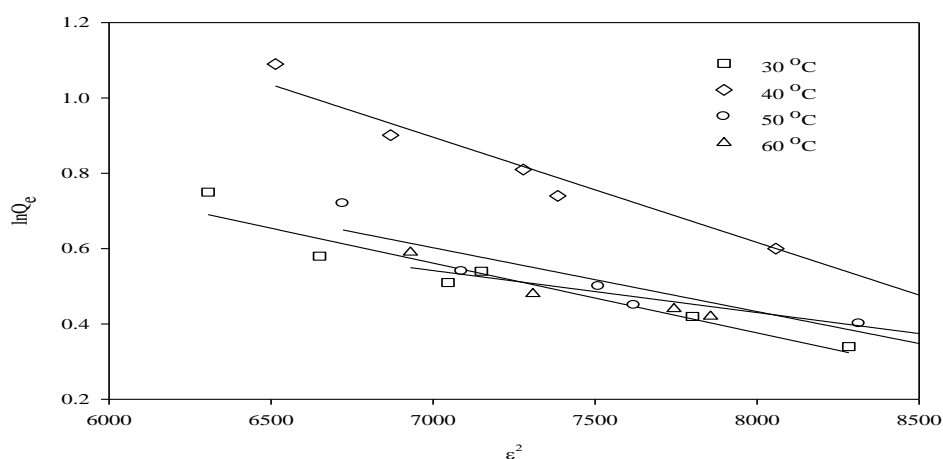
Figure 11: The linearized Dubinin-Kaganer-Radushkevich (DKR) adsorption isotherm

Table 4: DKR adsorption constants and regression values at different temperatures

T ($^\circ$C)	β	X_m	E	R^2
30	-0.0002	6.4134	50.012	0.9201
40	-0.0003	17.3085	40.8248	0.9667
50	-0.0002	5.9810	50.213	0.8925
60	-0.0001	3.7520	70.7106	0.8945

4.4. Regeneration of Zeolite

Regeneration efficiency for cadmium reduced within the first 3 cycles to approximately 80–85% and to less than 50% after 9 regeneration cycles. Several reasons can be accounted for this behaviour. The reasons involved may be due to the presence of various impurities (such as carbonates) along with the free spaces of zeolite structure, which involves the cavities and various channels inside its structure which hinder the transport of the metal, i.e. cadmium to the ion exchange sites. The other reasons can be complexation between chloride and metals as a result the metals that are trapped inside and not providing passage for fresh incoming metals for the ion-exchange action [49-50]. The reduction in desorption efficiency during each cycle means that some heavy metals actually remained on the zeolite and therefore decreased the amount of metal adsorbed during the subsequent adsorption cycles.

Conclusion

Zeolite obtained from coal fly ash is an inexpensive and effective adsorbent for the removal of cadmium from wastewater. The effect of temperature, pH and adsorbent dosage on the adsorption of cadmium by zeolite was studied. Maximum adsorption has been found to be at pH 6, at 40 °C and at an adsorbent dosage of 2 g/100 mL. The change in the surface morphology of zeolite was observed from the SEM images. The adsorption data fit pretty well in both the Langmuir and Freundlich adsorption isotherms. The adsorption data also fit pretty well into DKR isotherm which has been used to find the mean energy of sorption which indicates ion exchange mechanism. Regeneration operations performed indicate that the zeolite can be effectively be used for five complete cycles without the loss of adsorption efficiency.

References

1. Sebastian, M., Olmo, I.F., Irabien, A., *Cem. Concr. Res.* 33 (2003) 1137.
2. Vinod, G.K., Rastogi, A., Diwivedi, M.K., Mohan, D., *Sep. Sci. Technol.* 32 (1997) 2883.
3. Somerset, V.S., Petrik, L.F., White, R.A., Klink, M.J., Key, D., Iwuoha, E.I., *Fuel* 84 (2005) 2324.
4. National Research Council, In: Catalysis Looks to the Future, (Panel on New Directions in Catalytic Science and Technology), National Academy Press, Washington D.C. (1992).
5. Molina, A., Poole, C., *Miner. Eng.* 17 (2004) 167.
6. Clement, R.E., Eiceman, G.A., Koester, C.J, *Anal. Chem.* 67 (1995) 221.
7. MacCarthy, P., Klusman, R.W., Cowling, S.W., Rice, J.A., *Anal. Chem.* 67 (1995) 525.
8. Zuane, J.D., Hand book of drinking water quality: standards and control, New York: Van Nostrand Reinhold (1990).

9. Weber, W.J., McGingley, P.M., Katz, L.E., *Water Res.* 25 (1991) 499.
10. Chu, K.H., Hasim, M.A., Shang, S.M., Sammel, V.B., *Water Sci. Technol.* 35 (1997) 115.
11. Venkatesham, V., Madhu, G.M., Satyanarayana, S.V., Preetham, H.S., *Chem. Prod. and Process Model.* 7(1) (2012).
12. Meena, A.K., Kadirvelu, K., Mishra, G.K., Rajagopal, C., Nagar, P.N., *J. Hazard. Mater.* 150 (2008) 604.
13. Huang, C.P., Rhoads, E.A., *J. Colloid Interface Sci.* 131 (1989) 230.
14. Argun M.E., Dursun S.A., *Bioresour. Technol.* 99 (2008) 2516.
15. Forstner U., Wittmann G.T.W., Metal transfer between solid and aqueous phases. In: Metal pollution in the aquatic environment. New York: Springer, (1979) 97.
16. Low, K.S., Lee, C.K., *Bioresour. Technol.* 38 (1991) 1.
17. Quasif, H., Yousfi, S., Bouamrnai, M.L., Kouali, M.E., Benmokhtar, S., Talbi, M., *J. Mater. Environ. Sci.* 4 (2013) 1.
18. Haddad, M.E, Mamouni, R., Slimani, R., Saffaj, N., Riadoui, M., ElAntri , S., Lazar, S., *J. Mater. Environ. Sci.* 3 (6) (2012) 1019.
19. Pollard, S.J.T., Fowler, G.D., Sollars, C.J., Perry, R., *Sci. Total Environ.* 116 (1992) 31.
20. Aly, H.M., Daifullah, A.A.M., *Adsorp. Sci. Technol.* 16 (1998) 33.
21. Daneshvar, N., Salari, D., Aber S., *J. Hazard. Mater.* B94 (2002) 49.
22. Dimitrova, S.V., Mehandgiev, D.R., *Water Res.* 32 (1998) 3289.
23. Ferraiolo, G., Zilli, M., Converti, A., *J. Chem. Technol. Biotechnol.* 47 (1990) 281.
24. Periasamy, K., Namasivayam, C., *Ind. Eng. Chem. Res.* 33 (1994) 317.
25. Srivastava, S.K., Tyagi, R., Pant, N., *Water Res.* 23 (1989) 1161.
26. Galiatsatou, P., Metaxas, M., Kasselouri-Rigopoulou, V., *J. Hazard. Mater.* B91 (2002) 187.
27. Mathialagan, T., Viraraghavan, T., *J. Hazard. Mater.* B94 (2002) 291.
28. Panayotova, M., Velikov, B., *Journal Environment science health A Toxic Hazard. Subst. Environ. Engg.* 38 (2003) 545.
29. Keane, M.A., *Colloid Surf. A* 138 (1998) 11.
30. Langella, A., Pansini, M., Cappelletti, P., de Gennaro, B., de GennaroM., Colella, C., *Micropor. Mesopor. Mater.* 37 (2000) 337.
31. Kim, J.S., Zhang, L., Keane, M.A., *Sep. Sci. Technol.* 37 (2001) 1509.
32. Biˇskup, B., Subotić, B., *Sep. Purif. Technol.* 37 (2004) 17.
33. Shawabkeh, R., Al-Harahsheh, A., Hami, M., Khlaifat, A., *Fuel* 83 (2004) 981.
34. Dal Bosco, S.M., Jimenez, R.S., Carvalho, W.A., *J. Colloid Interf. Sci.* 281 (2005) 424.
35. El-Kamash, A.M., Zaki, A.A., Abed El Geleel, M., *J. Hazard. Mater.* 127 (2005) 211.
36. Bein, T., In: Cejka, J., Van Bekkum, H., Corma, A., Schuth, F., (eds) Introduction to Zeolite Science and Practice, 3rd revised edn. Elsevier, (2007) 611.
37. Yilmaz, B., Sacco, A., Deng, J., *Appl. Phys. Lett.* 90 (2007) 152101.
38. Sakaguchi, K., Matsui, M., Mizukami, F., *Appl. MicroBiotechnol.* 67 (2005) 306.
39. Lee, M.G., Yi, G., Ahn, B.J., Roddick, F., *Korean J. Chem. Eng.* 17 (2000) 325.
40. Erdem, E., Karapinar, N., Donat, R., *J. Colloid Interface Sci.* 280 (2004) 309.
41. Flanigen, E.M., Khatami, H., Szymanski, H.A., *Advances in Chem. Series.* 101(1974) 201.
42. Sen, A.K., De, A.K., *Water Res.* 21 (1987) 885.
43. Teker, M., Imamoglu, M., Saltabas, O., *Turk. J. Chem.* 23 (1999) 185.
44. Borah, D., Senapati, K., *Fuel* 85 (2006) 1929.
45. Pratap, C., Shigeru, K., Toshinori, K., Shigeo, S., *J. Hazard. Mater.* 162 (2009) 440.
46. Weber, W.J., Physiochemical processes for water quality control. Wiley: NewYork, (1972) 208.
47. Ahalya, N., Kanamadi, R.D., Ramachandra, T.V., *Electron. J. Biotechnol.* 8 (2005) 258.
48. Onyango, M.S., Kuchar, D., Kubota, M., Matsuda, H., *Ind. Eng. Chem. Res.* 46 (2007) 894.
49. Boyd, G.E., Adamson, A.W., Meyers, L.S., *J. Am. Chem. Soc.* 69 (1947) 2836.
50. Reichenberg, D., *J. Am. Chem. Soc.* 75 (1953) 589.

(2013); http://www.jmaterenvironsci.com